

Shimada T, Yamaguchi N, Nishida N, Yamasaki K, Miura K, Katamine S, Masuzaki H.	Human Papillomavirus DNA in Plasma of Patients with HPV16 DNA-positive Uterine Cervical Cancer.	Jpn J Clin Oncol	in press		2010
Miura K, Miura S, Yoshiura K, Seminara S, Hamaguchi D, Niikawa N, Masuzaki H.	A case of Kallmann syndrome carrying a missense mutation in alternatively spliced exon 8A encoding the immunoglobulin-like domain IIIb of FGFR1.	Human Reproduction	25	1076-1080	2010
三浦清徳、増崎英明	Nuchal translucency: NT	長崎市医師会報	43 卷(11 号)	32-34	2009
三浦清徳、山崎健太郎、三浦生子、中山大介、増崎英明	TTTS のリスクを推定する分子診断法の確立を目指して-母体血漿中胎盤由来 mRNA を用いた検討-	日本産婦人科・新生児血液学会誌	18	107-113	2009
三浦清徳	Severe preterm IUGR における confined placental mosaicism の関与-特に周産期から出生後 12 ヶ月について	第 27 回周産期シンポジウム記録集		29	2009
谷川輝美、三浦清徳、吉田敦、中山大介、増崎英明	胎児死亡例からみた常位胎盤早期剥離の検討	日本産婦人科・新生児血液学会誌	18	13-17	2009
中山大介、三浦清徳、増崎英明	地域における母体救急搬送体制と問題点 5	長崎県 臨床婦人科産科	64 (1)	82-87	2010

## 研究成果の刊行物・別冊

# 平成19年度研究成果の刊行物・別冊

## Congenital Arhinia: Molecular-Genetic Analysis of Five Patients

**Daisuke Sato,<sup>1,2,3</sup> Osamu Shimokawa,<sup>1,3,4</sup> Naoki Harada,<sup>3,4</sup> Oystein E. Olsen,<sup>5</sup> Jia-Woei Hou,<sup>6</sup>  
Wolfgang Muhlbauer,<sup>7</sup> Ellen Blinkenberg,<sup>8</sup> Nobuhiko Okamoto,<sup>9</sup> Akira Kinoshita,<sup>1</sup>  
Naomichi Matsumoto,<sup>3,10</sup> Shinji Kondo,<sup>3,11</sup> Tatsuya Kishino,<sup>3,11</sup> Nobutomo Miwa,<sup>1,3</sup>  
Tadashi Ariga,<sup>2</sup> Norio Niikawa,<sup>1,3</sup> and Koh-ichiro Yoshiura<sup>1,3\*</sup>**

<sup>1</sup>Department of Human Genetics, Nagasaki University Graduate School of Biomedical Sciences, Nagasaki, Japan

<sup>2</sup>Department of Pediatrics, Hokkaido University Graduate School of Medicine, Sapporo, Japan

<sup>3</sup>Solution Oriented Research of Science and Technology (SORST), Japan Science and Technology Agency (JST), Kawaguchi, Japan

<sup>4</sup>Kyushu Medical Science, Nagasaki, Japan

<sup>5</sup>Department of Radiology, Great Ormond Street Hospital for Children, London, UK

<sup>6</sup>Division of Medical Genetics, Department of Pediatrics, Chang Gung Children's Hospital, Taoyuan, Taiwan

<sup>7</sup>Plastic Surgery Arabella, Munich, Germany

<sup>8</sup>Center for Medical Genetics and Molecular Medicine, Haukeland University Hospital, Bergen, Norway

<sup>9</sup>Department of Planning and Research, Osaka Medical Center and Research Institute for Maternal and Child Health, Izumi, Japan

<sup>10</sup>Department of Human Genetics, Yokohama City Graduate School of Medicine, Yokohama, Japan

<sup>11</sup>Division of Functional Genomics, Center for Frontier Life Sciences, Nagasaki University, Nagasaki, Japan

Received 30 May 2006; Accepted 30 October 2006

Congenital arhinia, complete absence of the nose, is an extremely rare anomaly with unknown cause. To our knowledge, a total of 36 cases have been reported, but there has been no molecular-genetic study on this anomaly. We encountered a sporadic case of congenital arhinia associated with a de novo chromosomal translocation, t(3;12)(q13.2;p11.2). This led us to analyze the patient by BAC-based FISH for translocation breakpoints and whole-genome array CGH for other possible deletions/duplications in the genome. We found in this patient an approximately 19 Mb deletion spanning from 3q11.2 to 3q13.31 but no disruption of any gene(s) at the other breakpoint, 12p11.2. As the deleted segment at 3q was a strong candidate region containing the putative arhinia gene, we also performed the

array CGH in four other arhinia patients with normal karyotypes, as well as mutation analysis of two genes, *COL8A1* and *CPOX*, selected among hundreds of genes located to the deleted region, because they are expressed during early stages of human craniofacial development. However, in the four patients, there were no copy number aberrations in the region examined or no mutations in the two genes. Although our study failed to identify the putative arhinia gene, the data may become a clue to unravel the underlying mechanism of arhinia. © 2007 Wiley-Liss, Inc.

**Key words:** arhinia; translocation breakpoint; deletion; 3q; 12p; FISH; array CGH

**How to cite this article:** Sato D, Shimokawa O, Harada N, Olsen OE, Hou J-W, Muhlbauer W, Blinkenberg E, Okamoto N, Kinoshita A, Matsumoto N, Kondo S, Kishino T, Miwa N, Ariga T, Niikawa N, Yoshiura K-i. 2007. Congenital arhinia: Molecular-genetic analysis of five patients. *Am J Med Genet Part A* 143A:546–552.

### INTRODUCTION

Congenital arhinia, complete absence of the nose, is an extremely rare abnormality with unknown cause. Congenital arhinia is often associated with microphthalmia, choanal atresia, and/or cleft palate [Graham and Lee, 2006]. To the best of our knowledge, only 36 cases of arhinia have been reported [Ruprecht and Majewski, 1978; Kaminker et al., 1985; Cohen and Goitein, 1986; Sakai et al., 1989; Galetti et al., 1994; Onizuka et al., 1995; Thiele et al., 1996;

Grant sponsor: Grants-in-Aid for Scientific Research; Grant number: 13854024; Grant sponsor: Applied Genomics; Grant numbers: 17019055, 17590288; Grant sponsor: Ministry of Education, Culture, Sports, Science and Technology (MEXT) of Japan; Grant sponsor: SORST (Japan Science and Technology Agency, JST).

\*Correspondence to: Koh-ichiro Yoshiura, MD, PhD, Department of Human Genetics, Nagasaki University Graduate School of Biomedical Sciences, Sakamoto 1-12-4, Nagasaki 852-8523, Japan.

E-mail: kyoshi@net.nagasaki-u.ac.jp

Published online 15 February 2007 in Wiley InterScience

(www.interscience.wiley.com)

DOI 10.1002/ajmg.a.31613

Choi et al., 1998; Cusick et al., 2000; Olsen et al., 2001; McGlone, 2003; Hou, 2004; Jules et al., 2004; Mathur et al., 2005; Shino et al., 2005; Graham and Lee, 2006]. Most cases were sporadic, but two familial cases were also reported [Ruprecht and Majewski, 1978; Thiele et al., 1996]. As two sisters with arhinia and microphthalmia were born to non-consanguineous parents, an autosomal recessive mode of inheritance has been suggested in this family [Ruprecht and Majewski, 1978]. In the other family, an aunt and a niece were affected with arhinia, suggesting a dominant mode of inheritance with reduced penetrance [Thiele et al., 1996]. Of the 17 patients who were karyotyped, 14 had a normal karyotype, whereas three cases had 46,XX/47,XX,+9 [Kaminker et al., 1985], inv(9) [Cohen and Goitein, 1986], or t(3;12)(q13.2;p11.2) [Hou, 2004]. These findings may indicate that genetic factors play a role in the occurrence of arhinia. Several genes have been proposed as candidates for arhinia, such as *PAX6* and its downstream targets, those of the FGF signaling, *MSX1*, *NRP2*, *GSC*, *ALX3*, and *ALX4* [Hou, 2004; Graham and Lee, 2006]. However, no genetic analysis has yet been undertaken. A de novo balanced reciprocal chromosomal translocation with a congenital disorder provides a good opportunity to discover the gene causing the disease [Mizuguchi et al., 2004].

We previously encountered a patient with congenital arhinia, small eyes and other abnormalities who was cytogenetically diagnosed to have a

translocation, t(3;12)(q13.2;p11.2) [Hou, 2004]. Under a hypothesis that a gene responsible for arhinia is disrupted at either of the breakpoints of the translocation, we performed breakpoint analysis of the patient as well as genome analyses of four other patients with arhinia.

## MATERIALS AND METHODS

### Subjects

This study was approved by the Committee for Ethical Issues on Human Genome and Gene Analysis, Nagasaki University. Five patients with arhinia were collected and analyzed as a collaboration study among six medical institutions (Nagasaki University Graduate School of Biomedical Sciences, Nagasaki, Japan; Great Ormond Street Hospital for Children, London, UK; Chang Gung Children's Hospital, Taoyuan, Taiwan; Plastic Surgery Arabella, Munich, Germany; Center for Medical Genetics and Molecular Medicine, Haukeland University Hospital, Bergen, Norway; and Osaka Medical Center and Research Institute for Maternal and Child Health, Osaka, Japan). Clinical findings of these five patients are shown in Table I. One patient (Patient A) had a de novo translocation, t(3;12)(q13.2;p11.2) and the other four patients (Patients B–E) were karyotypically normal.

We first focused our interest on Patient A and carried out a breakpoint analysis to try to isolate the

TABLE I. Clinical Findings of Five Patients With Arhinia

Clinical findings	Patients [References]				
	A	B	C	D	E
	[Hou, 2004]	[Okamoto, unpublished]	[Muhlbauer et al., 1993]	[Olsen et al., 2001]	[Sakai et al., 1989]
Sex	F	M	F	F	M
Karyotype	46,XX,t(3;12)(q13.2;p11.2)	46,XY	46,XX	46,XX	46,XY
High arched palate	+	+	+	+	+
Hypertelorism	+	+	+	+	+
Microphthalmia	Bilateral	Left	NA	NA	–
Coloboma iris	+	Left	NA	Bilateral	–
Published	–	–	–	–	–
Development	NA	N	N	N	N
Brain imaging	N	N	N	N	N
Olfactory bulbs	–	–	NA	–	NA
Family history	–	–	–	–	–
Pregnancy	UN	UN	UN	PH	NA
Birth weight (g)	2,800	2,368	2,640	3,070	3,346
Paranasal sinuses	UD	+	–	–	NA
Nasolacrimal ducts	NA	–	–	–	–
Complications	Scoliosis, epilepsy	Hypogonadism, autism	–	–	–
Current status	Living	Living	Living	Unknown	Living
	DD		ND		
	GR		GR		
			NNB		

F, female; M, male; +, observed; –, not observed; NA, not assessed; N, normal; UN, uneventful; PH, polyhydramnios; UD, underdeveloped; DD, delayed development; ND, normal development; GR, growth retardation; NNB, no nasal breathing.

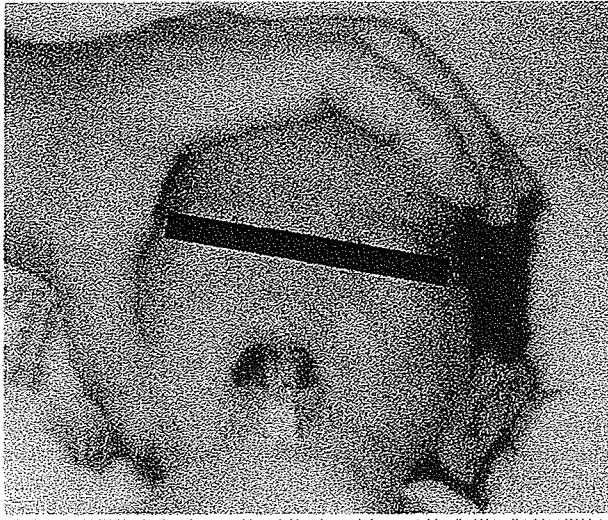


FIG. 1. Patient B at age 6 days, showing the absence of the nose.

putative arhinia gene. Detailed clinical features of Patients A, C, D, and E were reported previously [Sakai et al., 1989; Muhlbauer et al., 1993; Olsen et al., 2001; Hou, 2004, respectively]. Patient B was a Japanese boy whose clinical manifestations have been unpublished. He was born to healthy and non-consanguineous parents by cesarean at 39 weeks of gestation with a birth weight of 2,368 g, length 48 cm, and OFC of 33.7 cm (Fig. 1). Because of his congenital arhinia, a nasal airway was created by a surgical operation at age 17 days to facilitate oral feeding. Other clinical manifestations included bilateral microphthalmia, coloboma of the iris, mid-face hypoplasia, high arched palate, hypertelorism,

and absent nasolacrimal ducts. He had neither cleft palate nor low set ears. At age 4 years, his weight was 12.7 kg, height 94.7 cm, and OFC 50 cm, and had paranasal sinuses, normal hearing acuity, autistic behavior, and hypogonadotropic hypogonadism. He is currently able to eat foods through his mouth by himself. His psychomotor developmental quotient was estimated at 65.

### Fluorescence In Situ Hybridization (FISH) Analysis

Metaphase chromosomes were prepared from an immortalized lymphoblastoid cell line according to the standard protocol [Shimokawa et al., 2005]. The RPCI-11 human BAC clones mapped around the breakpoints, 3q13.2 and 12p11.2, were selected and used for FISH analyses. Mapping information was retrieved from the UCSC genome browser, 2003 July version (<http://genome.ucsc.edu/cgi-bin/hgGateway>). BAC-clone DNA was extracted using an automatic DNA extraction system (Kurabo, Osaka, Japan) and labeled with SpectrumGreen-11-dUTP or SpectrumOrange-11-dUTP (Vysis, Downers Grove, IL) by nick translation. Fluorescent probes were hybridized to metaphase chromosomes for 16–72 hr, and then chromosome slides were washed and counterstained with DAPI using standard protocols [Shimokawa et al., 2005]. Fluorescence signals were observed under Zeiss Axioskop microscope equipped with a quad filter set with single-band excitation filters (84000, Chroma Technology Corporation, Brattleboro, VT). Images were captured by cooled CCD camera (TEA/CCD-1317-G1, Princeton Instruments, Trenton, NJ) and merged with IPLab/MA.

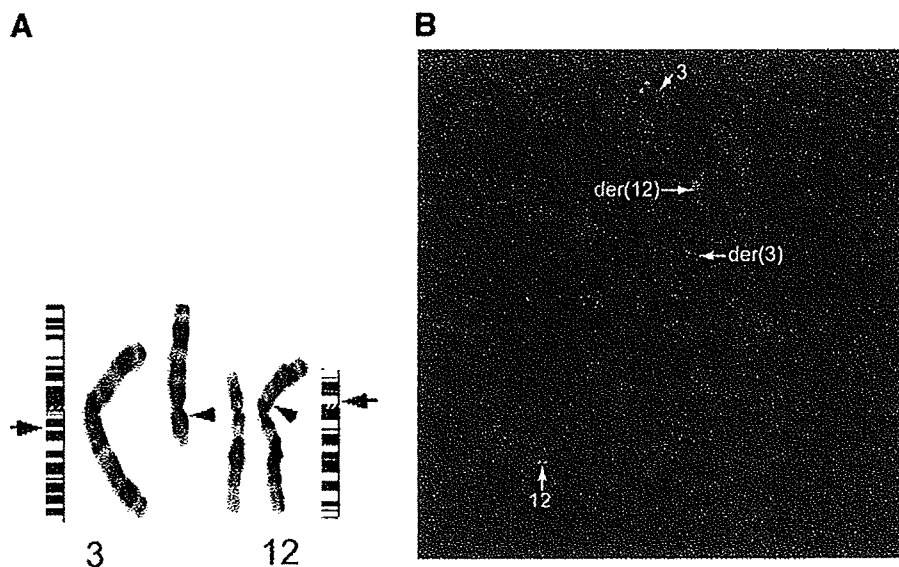


FIG. 2. A: Partial karyotype of Patient A. Arrows and arrowheads show the breakpoints. B: FISH analysis in Patient A. Green signals for a BAC clone, RP11-55L17, that spans the 12p breakpoint appear on der(3), der(12) and normal chromosome 12, while red signals for a chromosome 3-derived clone, RP11-803P6, are seen only on normal chromosome 3. The findings indicate a deletion only in der(3).

### Array Comparative Genomic Hybridization (CGH)

DNA was extracted from peripheral blood lymphocytes by conventional method [Sambrook and Russell, 2001]. To detect chromosomal aberrations, we performed homemade whole-genome BAC-based array CGH (array CGH) using genomic DNA of all five patients according to the method described previously [Miyake et al., 2006]. The microarray contains 2,173 BAC and PAC clones which span the whole genome at each of 1.5 Mb average.

### Mutation Analysis

A screening for mutations of *COL8A1* and *CPOX* was performed in the four arhinia patients with normal karyotypes. All exon sequences and their flanking intron sequences of the two genes were

amplified by PCR for direct sequencing. PCR conditions were set at 40 cycles of 94°C for 30 sec, 62°C for 30 sec, and 72°C for 45 sec in a 15 µl mixture containing 1 × PCR buffer with 1.5 mM MgCl<sub>2</sub>, 0.2 mM each of dNTP, 1 µM each primer and 0.4 Units Taq polymerase (TaKaRa, Otsu, Japan). PCR products were treated with ExoSAP-IT (Amersham Biosciences, Piscataway, NJ) and both strands were sequenced with BigDye Terminator Sequencing kit version 3.1 according to the supplied protocol (Applied Biosystems, Foster City, CA). The reaction mixture was purified using Sephadex G-50 superfine (Amersham Biosciences) and analyzed on the ABI Genetic Analyzer 3100 (Applied Biosystems) with the Sequence Analysis software (Applied Biosystems) and aligned with the Auto Assembler version 2.1.1 software (Applied Biosystems) to find DNA alterations.

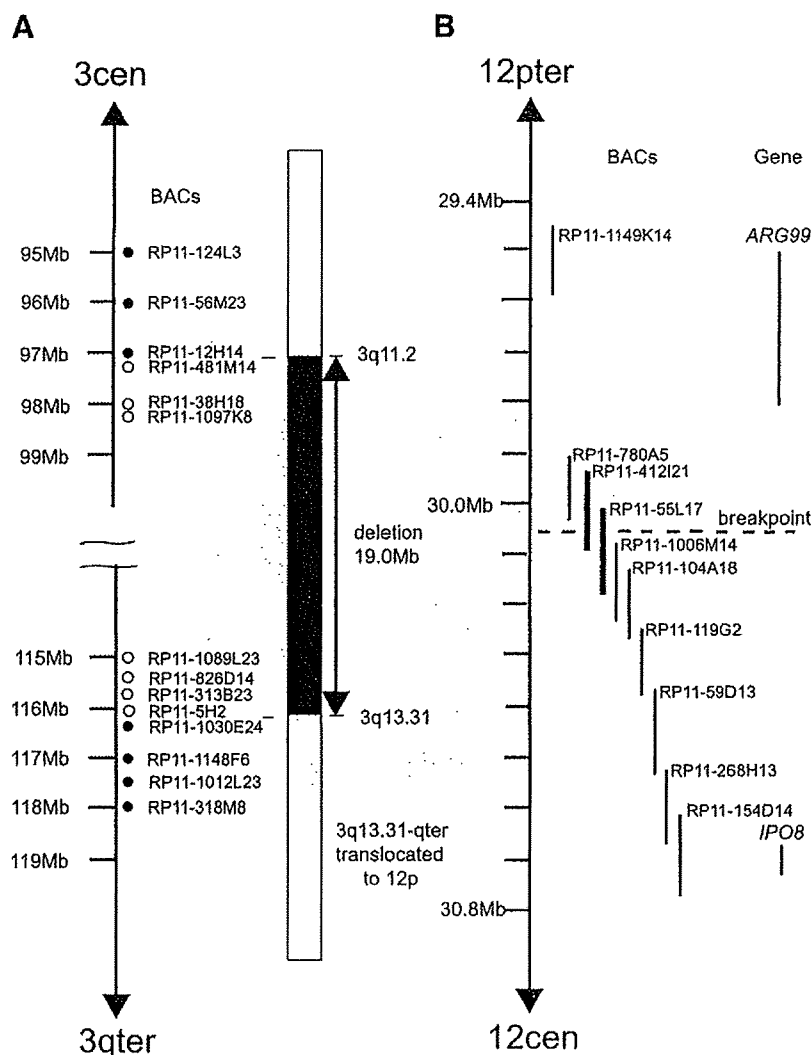


FIG. 3. **A:** Physical map covering the 3q11.2–3q13.31 deleted region of Patient A. Solid and open circles indicate the presence and absence of clones in Patient A, respectively. **B:** Physical map of the 12p11 breakpoint region. Thick lines indicate BAC clones covering the breakpoint. Genes *ARG99* and *IPO8* are located close to the breakpoint.

## RESULTS AND DISCUSSION

Although the translocation of Patient A looked balanced (Fig. 2A) [Hou, 2004], there was actually a relatively large deletion at the 3q13.2 breakpoint region of her derivative chromosome 3. FISH analysis revealed that the 3q proximal end of the deleted segment was confined to 3q11.2 between BAC clones, RP11-12H14, and RP11-481M14, and the distal end to 3q13.31 between RP11-5H2 and RP11-1030E24 (Figs. 2B and 3). Since lacking signals were confirmed for 16 other BACs that are located between the two ends, the deletion extended to approximately 19 Mb in size from 3q11.2 to 3q13.31 (UCSC Genome Browser). As for the other derivative chromosome 12, as two neighbor BAC clones, RP11-412I21, and RP11-55L17, in a contig were identified to cover the 12p11.22 breakpoint, there was no deletion at the breakpoint.

To know whether any other chromosomal aberrations exist in the genome of the five patients examined, whole-genome array CGH was performed. Consequently, the array CGH confirmed in Patient A the presence of the 3q deletion (Fig. 4) without deletions or duplications in any other chromosomes. In Patient D, four regions were suspected to have duplication, but this could not be confirmed by subsequent FISH, because her chro-

mosome preparation was not available. There was no chromosomal aberration in the remaining three patients.

A literature search for deletions for 3q11.2–3q13.31 found eight reported cases [Arai et al., 1982; Jenkins et al., 1985; McMorroo et al., 1986; Okada et al., 1987; Fujita et al., 1992; Genuardi et al., 1994; Ogilvie et al., 1998]. The smallest region of overlap (SRO) for deletion among them is almost confined to 3q12–3q13.31 (Fig. 5). The deletion in one patient (Case 8 in Fig. 5) [Jenkins et al., 1985] was reported to lie between 3q11 and 3q21. However, the exact location of the proximal border in this patient was not clear since either FISH or molecular analysis was not carried out. None but one patient [Arai et al., 1982] had any nose anomaly, and none of the eight patients manifested microphthalmia that is virtually accompanied with arhinia [Graham and Lee, 2006]. The exceptional patient whose deletion involved 3q13–q21 (Case 7, Fig. 5) had alobar holoprosencephaly, arhinia, and cleft lip [Arai et al., 1982]. Although arhinia of this case seems atypical and to be a holoprosencephaly-associated median facial anomaly, the patient might provide possible information for localization of the arhinia locus. If the locus exists at the long arm of chromosome 3, it might be confined to a segment between 3q11.2 and the proximal border of the deletion of Case 8

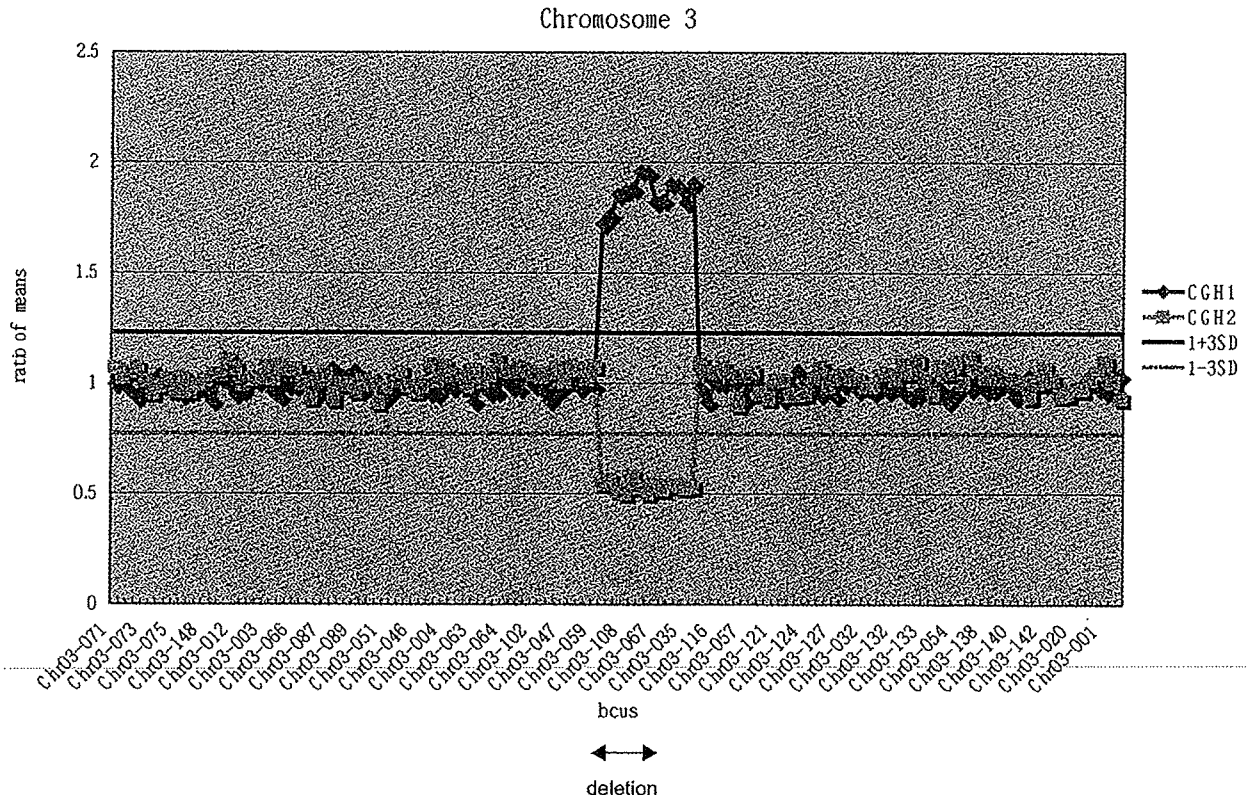


FIG. 4. Array CGH analysis in Patient A, showing a deletion on 3q. The clone at the proximal end within the deletion was RP11-262O19 (3q11.2), and the distal end clone was RP11-342J15 (3q13.31), the results suggesting that the deletion is approximately 18 Mb in size.



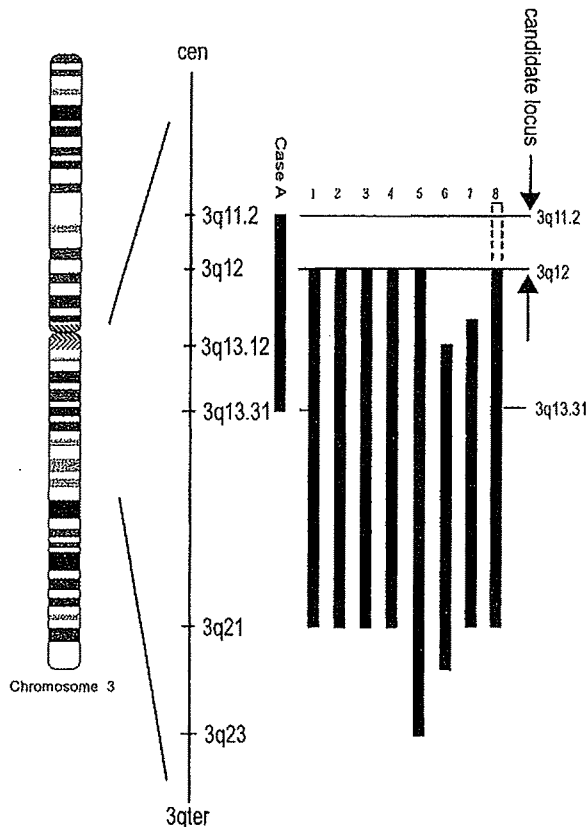


FIG. 5. Extent (bars) of 3q11.2–3q13.31 deletion in Patient A and eight reported cases. Lanes 1–8 are from McMorrow et al. [1986], Ogilvie et al. [1998], Okada et al. [1987], Fujita et al. [1992], Genuardi et al. [1994], Arai et al. [1982], and Jenkins et al. [1985], respectively.

(Fig. 5). We selected two genes, *COL8A1* and *CPOX*, from 3q11.2 within the deletion of Patient A, and analyzed for their mutations in Patients B–E. According to the Craniofacial and Oral Gene Expression Network (COGENE, <http://hg.wustl.edu/COGENE/index.html>), *COL8A1* and *CPOX* are expressed in the frontonasal prominence at the 4th week, and between the 4th and 5th weeks, respectively, suggesting they play some roles in the nasal development. However, there was no pathogenomic mutation of *COL8A1* or *CPOX* in the four arhinia patients with normal karyotypes.

As for the other breakpoint of Patient A, we have confirmed that any known genes were not disrupted at 12p11.22. Two genes, *ARG99* and *IPO8*, located near the breakpoint, seem to have no functions related to the human nasal development. However, it cannot totally be ruled out that there may be unknown RNA transcript(s) on the breakpoint or the breakage may affect a long-distance position effect [Velagaleti et al., 2005].

The nasal placode, the anlage of the nose, begins to develop from the 12th to the 13th Carnegie stage, at the end of the fourth embryonic week. The stage between the end of the 4th week to the 7th week is

the most active, important period in the human nose development [O'Rahilly, 1967; Kim et al., 2004]. A failure of the developmental process may result in arhinia, for example, failure of growth or overgrowth of the medial and lateral nasal process sequentially leads to premature fusion of the medial nasal processes [Albernaz et al., 1996].

In conclusion, analysis of five patients with arhinia revealed, although a 19 Mb large deletion involving 3q11–q13 was identified in one patient, no chromosome aberrations or gene mutations were found in the other four patients. Nevertheless, our findings may become a clue to isolate the putative arhinia gene. Further molecular studies in new patients, as well as that on other genes within the deleted region in Patient A, are needed to unravel the underlying cause of arhinia. This is the first report of molecular-genetic study on congenital arhinia.

#### ACKNOWLEDGMENTS

Participation of all patients in this study is highly appreciated. We also thank Ms Y. Noguchi, K. Miyazaki and A. Goto for their technical assistance. This study was supported by Grants-in-Aid for Scientific Research (Category S, No. 13854024 and Priority Areas—Applied Genomics, No. 17019055 for N. N.; and No. 17590288 for K. Y.) from the Ministry of Education, Culture, Sports, Science and Technology (MEXT) of Japan, and by SORST from the Japan Science and Technology Agency (JST) for N. N.

#### REFERENCES

- Albernaz VS, Castillo M, Mukherji K, Ihmeidan IH. 1996. Congenital arhinia. *Am J Neuroradiol* 17:1312–1314.
- Arai K, Matukiyo H, Takazawa H. 1982. A case report of partial deletion of the long arm of the No.3 chromosome. *Med Genet Res* 4:1–4.
- Choi S, Shiozu H, Sato K, Nishida H. 1998. A case report of congenital arhinia. *Acta Neonatol Jpn* 34:83–86.
- Cohen D, Goitein K. 1986. Arhinia. *Rhinology* 24:287–292.
- Cusick W, Sullivan CA, Rojas B, Poole AE, Poole DA. 2000. Prenatal diagnosis of total arhinia. *Ultrasound Obstet Gynecol* 15:259–261.
- Fujita H, Meng J, Kawamura M, Tozuka N, Ishii F, Tanaka N. 1992. Boy with a chromosome del(3)(q12q23) and blepharophthalmos syndrome. *Am J Med Genet* 44:434–436.
- Galetti R, Dallari S, Bruzzi M, Vincenzi A, Galetti G. 1994. Consideration on respiratory physiopathology in a case of total arhinia. *Acta Otorhinol Ital* 14:63–69.
- Genuardi M, Calvieri F, Tozzi C, Coslovi R, Neri G. 1994. A new case of interstitial deletion of chromosome 3q, del(3q)(q13.12q21.3), with agenesis of the corpus callosum. *Clin Dysmorphol* 3:292–296.
- Graham JM, Lee J. 2006. Bosma arhinia microphthalmia syndrome. *Am J Med Genet Part A* 140A:189–193.
- Hou JW. 2004. Congenital arhinia with de novo reciprocal translocation, t(3;12)(q13.2;p11.2). *Am J Med Genet Part A* 130A:200–203.
- Jenkins MB, Stang HJ, Davis E, Boyd L. 1985. Deletion of the proximal long arm of chromosome 3 in an infant with features of Turner syndrome. *Ann Génét (Paris)* 28:42–44.

- Jules AF, Cynthia MG, Terry T, Samue S, Brian S, Larry H. 2004. Vertical facial distraction in the treatment of arhinia. *Plast Reconstr Surg* 113:2061–2066.
- Kaminker CP, Dain L, Lamas MA, Sanchez JM. 1985. Mosaic trisomy 9 syndrome with unusual phenotype. *Am J Med Genet* 22:237–241.
- Kim CH, Park HW, Kim K, Yoon JH. 2004. Early development of the nose in human embryos: A stereomicroscopic and histologic analysis. *Laryngoscope* 114:1791–1800.
- Mathur NN, Dubey NK, Kumar S, Bothra R, Chadha A. 2005. Arhinia. *Int J Pediatr Otorhinolaryngol* 69:97–99.
- McGlone L. 2003. Congenital arhinia. *J Paediatr Child Health* 39:474–476.
- McMorrow LE, Reid CS, Coleman J, Medeiros A, D'Andrea M, Santucci T, McCormack MK. 1986. A new interstitial deletion of the long arm of chromosome 3. *Am J Hum Genet* 39:A124.
- Miyake N, Shimokawa O, Harada N, Sosonkina N, Okubo A, Kawara H, Okamoto N, Ohashi H, Kurosawa K, Naritomi K, Kaname T, Nagai T, Shotelersuk V, Hou JW, Fukushima Y, Kondoh T, Matsumoto T, Shinoki T, Kato M, Tonoki H, Nomura M, Yoshiura K, Kishino T, Ohta T, Niikawa N, Matsumoto N. 2006. No detectable genomic aberrations by BAC array CGH in Kabuki make-up syndrome patients. *Am J Med Genet Part A* 140A:291–293.
- Mizuguchi T, Collod-Beroud G, Akiyama T, Harada N, Morisaki T, Abifadel M, Allard D, Varret M, Claustres M, Ihara M, Kinoshita A, Yoshiura K, Junien C, Kajii T, Jondeau G, Niikawa N, Boileau C, Matsumoto N. 2004. Heterozygous *TGFBR2* mutations in Marfan syndrome. *Nat Genet* 36:855–860.
- Muhlbauer W, Schmidt A, Fairley J. 1993. Simultaneous construction of an internal and external nose in an infant with arhinia. *Plast Reconstr Surg* 91:720–725.
- O'Rahilly R. 1967. The early development of the nasal pit in staged human embryos. *Anat Rec* 157:380.
- Ogilvie CM, Rooney SC, Hodgson SV, Berry AC. 1998. Deletion of chromosome 3q proximal region gives rise to a variable phenotype. *Clin Genet* 53:220–222.
- Okada N, Hasegawa T, Osawa M, Fukuyama Y. 1987. A case of de novo interstitial deletion 3q. *J Med Genet* 24:305–308.
- Olsen OE, Gjelland K, Reigstad H, Rosendahl K. 2001. Congenital absence of the nose: A case report and literature review. *Pediatr Radiol* 31:225–232.
- Onizuka T, Ohkubo F, Hosaka Y, Ichinose M, Keiko Okazaki K. 1995. Arhinia: A case report. *Worldplast* 1:65–71.
- Ruprecht KW, Majewski F. 1978. Familial arhinia combined with Peter's anomaly and maxillar deformities, a new malformation syndrome? *Klin Mbl Augenheilk* 172:708–715.
- Sakai Y, Ohara Y, Inoue Y. 1989. Congenital complete absence of the nose. *J Jpn Plast Reconstr Surg* 9:265–273.
- Sambrook J, Russell DW. 2001. *Molecular cloning: A laboratory manual*. Cold Spring Harbor, New York: Cold Spring Harbor Laboratory Press.
- Shimokawa O, Miyake N, Yoshimura T, Sosonkina N, Harada N, Mizuguchi T, Kondoh S, Kishino T, Ohta T, Remco V, Takashima T, Kinoshita A, Yoshiura K, Niikawa N, Matsumoto N. 2005. Molecular characterization of del(8)(p23.1p23.1) in a case of congenital diaphragmatic hernia. *Am J Med Genet Part A* 136A:49–51.
- Shino M, Chikamatsu K, Yasuoka Y, Nagai K, Furuya N. 2005. Congenital arhinia: A case report and functional evaluation. *Laryngoscope* 115:1118–1123.
- Thiele H, Musil A, Nagel F, Majewski F. 1996. Familial arhinia, choanal atresia, and microphthalmia. *Am J Med Genet* 63:310–313.
- Velagaleti GVN, Bien-Willner GA, Northup JK, Lockhart LH, Hawkins JC, Jalal SM, Withers M, Lupski JR, Stankiewicz P. 2005. Position Effects due to chromosome breakpoints that map ~900 kb upstream and ~1.3 Mb downstream of SOX9 in two patients with Campomelic dysplasia. *Am J Hum Genet* 76:652–662.

## Role of DNA Methylation and Histone H3 Lysine 27 Methylation in Tissue-Specific Imprinting of Mouse *Grb10*<sup>V</sup>

Yoko Yamasaki-Ishizaki,<sup>1,2,8</sup> Tomohiko Kayashima,<sup>1</sup> Christophe K. Mapendano,<sup>1</sup> Hidenobu Soejima,<sup>3</sup> Tohru Ohta,<sup>4,8</sup> Hideaki Masuzaki,<sup>2</sup> Akira Kinoshita,<sup>1,8</sup> Takeshi Urano,<sup>5</sup> Ko-ichiro Yoshiura,<sup>1,8</sup> Naomichi Matsumoto,<sup>6</sup> Tadayuki Ishimaru,<sup>2</sup> Tsunehiro Mukai,<sup>3</sup> Norio Niikawa,<sup>1,8</sup> and Tatsuya Kishino<sup>7,8\*</sup>

Departments of Human Genetics<sup>1</sup> and Obstetrics and Gynecology,<sup>2</sup> Graduate School of Biomedical Sciences, Nagasaki University, Nagasaki, Japan; Department of Biomolecular Sciences, Saga University, Saga, Japan<sup>3</sup>; The Research Institute of Personalized Health Sciences, Health Sciences University of Hokkaido, Hokkaido, Japan<sup>4</sup>; Department of Biochemistry II, Graduate School of Medicine, Nagoya University, Nagoya, Japan<sup>5</sup>; Department of Human Genetics, Graduate School of Medicine, Yokohama City University, Yokohama, Japan<sup>6</sup>; Division of Functional Genomics, Center for Frontier Life Sciences, Nagasaki University, Nagasaki, Japan<sup>7</sup>; and CREST, Japan Science and Technology Agency, Kawaguchi, Japan<sup>8</sup>

Received 19 July 2006/Accepted 24 October 2006

Mouse *Grb10* is a tissue-specific imprinted gene with promoter-specific expression. In most tissues, *Grb10* is expressed exclusively from the major-type promoter of the maternal allele, whereas in the brain, it is expressed predominantly from the brain type promoter of the paternal allele. Such reciprocally imprinted expression in the brain and other tissues is thought to be regulated by DNA methylation and the Polycomb group (PcG) protein Eed. To investigate how DNA methylation and chromatin remodeling by PcG proteins coordinate tissue-specific imprinting of *Grb10*, we analyzed epigenetic modifications associated with *Grb10* expression in cultured brain cells. Reverse transcriptase PCR analysis revealed that the imprinted paternal expression of *Grb10* in the brain implied neuron-specific and developmental stage-specific expression from the paternal brain type promoter, whereas in glial cells and fibroblasts, *Grb10* was reciprocally expressed from the maternal major-type promoter. The cell-specific imprinted expression was not directly related to allele-specific DNA methylation in the promoters because the major-type promoter remained biallelically hypomethylated regardless of its activity, whereas gametic DNA methylation in the brain type promoter was maintained during differentiation. Histone modification analysis showed that allelic methylation of histone H3 lysine 4 and H3 lysine 9 were associated with gametic DNA methylation in the brain type promoter, whereas that of H3 lysine 27 regulated by the Eed PcG complex was detected in the paternal major-type promoter, corresponding to its allele-specific silencing. Here, we propose a molecular model that gametic DNA methylation and chromatin remodeling by PcG proteins during cell differentiation cause tissue-specific imprinting in embryonic tissues.

Genomic imprinting in mammals describes the situation where there is nonequivalence in expression between the maternal and paternal alleles at certain gene loci, depending on the parental origin. Genomic imprinting plays essential roles in development, growth, and behavior (6, 30, 31). Such parental origin-specific gene regulation is caused by epigenetic modifications that occur during gametogenesis without any nucleic acid changes. One of the well-known epigenetic modifications is DNA methylation. In the imprinted loci, differentially methylated regions between the maternal and paternal alleles are often found and associated with parental allele-specific expression (7). Another well-known epigenetic modification is histone modification, which represents the determinant of epigenetic features associated with imprinted genes. It has been reported that parental origin-specific gene expression on some imprinted genes is determined by DNA methylation and/or histone modifications (12, 13, 16, 23, 29, 40). Polycomb group

(PcG) proteins also play an important role in various epigenetic phenomena (3), such as maintaining the silent state of the homeotic genes, maintaining X-chromosome inactivation (36), and silencing imprinted genes in mammals (24, 33). PcG protein complexes are thought to maintain long-term gene silencing during development through alterations of local chromatin structure (3, 27).

Mouse *Grb10* encoding the growth factor receptor-bound protein 10 (Grb10) is an imprinted gene with tissue-specific and promoter-specific expression. In most tissues, the major-type transcript of *Grb10* is expressed exclusively from the major-type promoter of the maternal allele, whereas in the brain, the brain type transcript is expressed predominantly from the brain type promoter of the paternal allele (1, 17). DNA methylation analysis has revealed that the CpG island (CGI) in the brain type promoter (CGI2) was gametically methylated in the oocyte as a primary imprint and remained methylated exclusively on the maternal allele in somatic tissues, while the CpG island in the major-type promoter (CGI1) was biallelically hypomethylated in somatic tissues (see Fig. 1 and 4) (17). Hikichi et al. proposed the model for tissue-specific imprinting of *Grb10* that the major-type transcript is regulated by DNA methylation-sensitive insulator (CTCF) binding in CGI2 and

\* Corresponding author. Mailing address: Division of Functional Genomics, Center for Frontier Life Sciences, Nagasaki University, Sakamoto 1-12-4, Nagasaki 852-8523, Japan. Phone: 81-95-849-7120. Fax: 81-95-849-7178. E-mail: kishino@net.nagasaki-u.ac.jp.

<sup>V</sup> Published ahead of print on 13 November 2006.

the brain type transcript is regulated by putative brain-specific activators (17). They suggested that allelic DNA methylation in CGI2 can orchestrate reciprocal imprinting of the two promoters of the *Grb10* gene. This model was partially supported by the imprinting analysis of knockout mice of the *Dnmt3L* gene, encoding a factor for acquisition of maternal methylation imprint in germ cells (14, 18). In the embryos (*Dnmt3L<sup>m-/-</sup>*), produced from *Dnmt3L<sup>m-/-</sup>* females, maternal chromosome-specific DNA methylation in CGI2 was lost and null expression of the major-type transcript was detected (2). Recently, the PcG protein Eed (embryonic ectoderm development) was identified as a member of a new class of *trans*-acting factors, which regulate the expression of some paternally repressed imprinted genes, *Cdkn1c*, *Ascl2*, *Meg3*, and *Grb10* (24). In *Eed<sup>-/-</sup>* embryos, the major-type transcript of *Grb10* was biallelically expressed from the major-type promoter without major alteration of DNA methylation in gametically methylated CGI2, albeit various hypomethylated patterns were observed on the paternal allele (24). The expression analysis of these knockout mice suggests that DNA methylation and chromatin remodeling by PcG proteins represent the epigenetic factors that are necessary for establishing and/or maintaining the imprinted expression of *Grb10*. It remains unknown how they coordinate the tissue-specific and promoter-specific imprinting of *Grb10*.

Recently, mouse genes with brain-specific imprinting patterns were reported. They are *Ube3a* and *Murr1*, with neuron-specific and brain developmental stage-specific expressions, respectively. *Ube3a* is biallelically expressed in most tissues but expressed exclusively from the maternal allele only in neurons, leading to apparent partial imprinting with predominant maternal *Ube3a* expression in the whole brain (38). *Murr1* is imprinted in the adult brain, especially in mature neurons, but not in embryonic and neonatal brains (37). These lines of evidence suggest that brain-specific imprinting may be regulated in part by epigenetic modifications, depending on specification and maturation of cell lineages in the developing brain (9, 19).

Since *Grb10* is a tissue-specific imprinted gene, we hypothesized that tissue-specific reciprocal imprinting of *Grb10* also depends on cell-specific epigenetic modifications acquired during cell differentiation. To examine our hypothesis, we performed an epigenetic analysis of brain cells with the aid of primary cortical cell cultures, in which neurons or glial cells were cultured separately from products of reciprocal crosses between the C57BL/6 and PWK strains (divergent strains of *Mus musculus*). In each cultured brain cell, *Grb10* expression and epigenetic factors such as DNA methylation and histone modifications were analyzed to investigate how DNA methylation and chromatin remodeling by PcG proteins establish and maintain the tissue-specific and promoter-specific imprinting of *Grb10*.

#### MATERIALS AND METHODS

**Mice.** All procedures were performed with approval from the Nagasaki University Institutional Animal Care and Use Committee. F<sub>1</sub> hybrid mice were obtained by mating C57BL/6 females with PWK males [(C57BL/6 × PWK)F<sub>1</sub>] and vice versa [(PWK × C57BL/6)F<sub>1</sub>]. Telencephalon/cerebral cortices and embryonic fibroblasts were prepared from embryonic day 10 (E10) to E15. Tissues were used for RNA and DNA extraction or primary cultures. Brain tissue

for reverse transcriptase (RT) PCR was dissected at E10, E16, postnatal day 1, postnatal day 5, 2 weeks, 4 weeks, 6 weeks, and 14 months.

**Primary culture.** Methods of primary cultures of cortical neurons, glial cells, and embryonic fibroblasts have been described elsewhere (38). In brief, E15 cerebral cortices without meninges were trypsinized to dissociate brain cells. For neuronal culture, dissociated cells were cultured in neurobasal medium (Gibco BRL, Carlsbad, CA) with B27 supplement (Gibco BRL). Cultures were maintained in 5% CO<sub>2</sub> at 37°C for 5 days. For the long culture, half of the culture medium was changed every 3 to 4 days. For glial cell culture, dissociated brain cells were cultured overnight in Dulbecco's modified Eagle's medium (Sigma, St. Louis, MO) supplemented with 10% fetal calf serum, and then the medium was changed to Neurobasal medium (Gibco BRL) with G5 supplement (GIBCO BRL). After 5 to 7 days in the primary culture, cultured glial components were subcultured. Cultures were maintained in 5% CO<sub>2</sub> at 37°C for a total of 14 days. For embryonic fibroblast culture, embryonic fibroblasts derived from E15 embryonic skin were cultured in Dulbecco's modified Eagle's medium supplemented with 10% fetal calf serum.

**cDNA synthesis.** Total RNA was isolated from cultured cells and tissues with RNeasy (QIAGEN, Hilden, Germany) according to the manufacturer's protocol. The RNA was treated with amplification grade DNase I (Invitrogen, Carlsbad, CA) to degrade any genomic DNA present in the sample. The cDNA was generated from total RNA by SuperScript II reverse transcriptase (Invitrogen) primed with oligo(dT)<sub>12-18</sub> primers. The first-strand cDNA was synthesized at 42°C for 50 min. Then, mRNA-cDNA chains were denatured and the reverse transcriptase activity was arrested by heating at 70°C for 15 min. An identical reaction was carried out without reverse transcriptase as a negative control.

**RT-PCR for expression analysis.** The cDNA obtained was used to perform RT-PCR for expression analysis. The expression of each *Grb10* transcript was analyzed using primers 1aF and 1R for the major-type transcript and using primers 1bF and 1R for the brain type transcript. Other transcripts, including exon 1c, were amplified by primer sets 1cF/e2R and 1aF/1cR. PCR amplification with primers 1aF and 1R was performed for 32 to 35 cycles of 15 s at 96°C, 20 s at 60°C, and 60 s at 72°C, with primers 1bF and 1R for 32 to 38 cycles of 15 s at 96°C, 20 s at 60°C, and 60 s at 72°C, and with primer sets 1cF/e2R and 1aF/1cR for 35 cycles of 15 s at 96°C, 20 s at 60°C, and 60 s at 72°C. The primers for *Map2*, *Gfap*, and *Gapdh* used for evaluation of the cultured cells have been described elsewhere (38). For a semiquantitative RT-PCR, optimal template cDNA concentrations were determined according to *Gapdh* amplification. PCR products were amplified for 25 to 30 cycles of 15 s at 96°C, 20 s at 55°C, and 30 s at 72°C.

**Quantitative analysis of gene expression by real-time PCR.** cDNA was applied to real-time PCR for quantitative analysis of each transcript using SYBR green and an ABI Prism 7900 (PE Applied Biosystems, Foster City, CA). PCR was performed on samples at least in triplicate according to the manufacturer's protocol to control for PCR variation. To standardize each experiment, the results were represented as a percentage of expression, calculated by dividing the average value of the expression of the target gene by that of an internal control gene, *Gapdh* (38). The primers used for real-time PCR were primers 1aF and 1R for the major-type transcript and primers Q-1bF and Q-1bR for the brain type transcript. Each experiment was repeated with independent RNAs two to three times.

**Sequencing for allelic differences.** A sequence chromatogram was used to detect allelic differences of PCR products. Parental expression of major/brain type transcripts in the brain and kidney was analyzed by RT-PCR using primer sets 1aF/coR and 1bF/coR for 35 to 38 cycles of 15 s at 96°C, 20 s at 60°C, and 120 s at 72°C. Parental chromosome-specific histone modifications in the major-type promoter were analyzed by PCR using the primer set ChIP-F/ChIP-R for 30 cycles of 30 s at 95°C, 30 s at 58°C, and 30 s at 72°C. The PCR products were analyzed by direct sequencing with a BigDye Terminator cycle sequencing kit (PE Applied Biosystems) on an automated sequencer, the ABI Prism 3100 genetic analyzer (PE Applied Biosystems).

**DNA methylation analysis.** Isolated DNA was treated with sodium bisulfite using a CpGenome DNA modification kit (Chemicon International Inc., Temecula, CA) according to the manufacturer's protocol. Bisulfite-treated DNA samples were subjected to nested PCR amplification using the following first and second primer pairs, respectively, for each CGI; CGI1, Me1F/Me-1R and Me-1F'/Me-1R'; CGI2, Me-2F/Me-2R and Me-2F'/Me-2R'; and CGI3, Me-3F/Me-3R and Me-3F'/Me-3R'. After the first PCR using the first primer set, the products were used as templates for nested PCR using the second primer set. The nested PCR products were cloned into the TA cloning vector (Invitrogen), and at least 32 clones for each sample were sequenced.

**ChIP.** A chromatin immunoprecipitation (ChIP) assay was performed with a ChIP assay kit (Upstate Biotechnology, Lake Placid, NY) according to the manufacturer's protocol. In brief, the chromatin of cultured cells was prepared from ~1.0 × 10<sup>6</sup> cells and treated with formaldehyde to cross-link DNA to

TABLE 1. Primers used in this study

Function(s) and primer	Sequence (5'-3')	Annealing temp (°C) (PCR cycle no.) <sup>a</sup>
<b>Expression and imprinting analysis</b>		
1aF <sup>b</sup>	CACGAAGTTCCGCGCA	
1bF	GCGATCATTCGTCTCTGAGC	
1R <sup>b</sup>	AGTATCAGTATCAGACTGCATGTTG	
1cF	ATCGCCATCTACAGTTTCTG	
1cR	CAAGGTACAGAGCTAGGACG	
e2R	CTGGTTGGCTTCTTTGTGTGG	
coR	TACGGATCTGCTCATCTTCG	
ChIP-F	TCACTTTAGAAACCGGGCA	
ChIP-R	AAACTCGGGCTTGCTCA	
<b>Quantitative analysis</b>		
Q-1bF	TCATTCGTCTCTGAGCGGCA	
Q-1bR	ATACGTGTTACATGCGCCAA	
Q-ChIP1F	TCACTTTAGAAACCGGGCA	
Q-ChIP1R	AAACTCGGGCTTGCTCA	
Q-ChIP2F	GATCATTCGTCTCTGAGC	
Q-ChIP2R	ATGCGGCAACATGCGCTGACA	
<b>Hot-stop PCR and SSCP analysis</b>		
ChIP2F-1	TCATTCGTCTCTGAGCGGCA	60 (32)
ChIP2R-1	TCTGGAGCCTAGAGGAGCG	
ChIP2F-2	AAGCGCGTGCTGGTTTGTA	60 (35)
ChIP2R-2	ATACGTGTTACATGCGCCAA	
<b>DNA methylation analysis</b>		
CG11 1st		53 (35)
Me-1F	TGGGGTTTAATATTAAGTTTGA	
Me-1R	TTACATCTCTTAAATAAAACA	
CG11 2nd		53 (35)
Me-1F'	TGGGGTTTAATATTAAGTTTGA	
Me-1R'	AAATCACCTATAACTCTCCTAC	
CG12 1st		50 (40)
Me-2F	TGGAGTTTAGAGGAG	
Me-2R	AATAGTTATTTAGTAAGGG	
CG12 2nd		50 (10)
Me-2F'	TGGAGTTTAGAGGAG	
Me-2R'	TAAGTGAAGTAATATAGTT	
CG13 1st		53 (40)
Me-3F	AAAGAAGGTTTGGAGAGATTATTT	
Me-3R	CAAACAAAACCTACTATATTTAAATTTAAAC	
CG13 2nd		53 (10)
Me-3F'	AAGGTTTGGAGAGATTATTTTGGATT	
Me-3R'	TAATTTAAACTTAACACTATTTAAATACC	

<sup>a</sup> For expression and imprinting analysis, the annealing temperature and PCR cycle number depend on the combination of primers used for each analysis. See details in Materials and Methods. For quantitative analysis, the PCR conditions were decided according to the manufacturer's protocol.

<sup>b</sup> Also used for quantitative analysis.

protein in situ, sonicated to an average size of 0.5 kb, and immunoprecipitated with antibodies. Antibodies against acetyl histone H3 (H3Ac; catalog no. 06-599), acetyl histone H4 (H4Ac; catalog no. 09-866), Lys4 dimethylated histone H3 (H3mK4; catalog no. 07-030), Lys9 trimethylated H3 (H3me3K9; catalog no. 07-212), and Lys27 trimethylated H3 (H3mK27; catalog no. 07-449) were obtained from Upstate Biotechnology. The monoclonal antibody against Lys9 dimethylated histone H3 (H3me2K9) was developed previously (26). Immunoprecipitated samples without antibodies or with rabbit immunoglobulin G precipitation were used as negative controls for precipitations with specific antibodies in each experiment.

**Quantitative analysis of immunoprecipitated DNA by real-time PCR.** Immunoprecipitated DNA and input DNA were analyzed by real-time PCR using the same protocol as that used for gene expression analysis. For DNA immunoprecipitated with H3Ac, H4Ac, and H3mK4 antibodies, the quantitative value of immunoprecipitated DNA in each CGI was normalized by dividing the average value of each CGI by that of the internal control, *Gapdh*. For DNA immunoprecipitated with H3me2K9 and H3me3K9 antibodies, the average value of *D13Mit55* was used instead of the value of *Gapdh*. Each normalized value of immunoprecipitated DNA was further divided by the normalized value of the

corresponding input DNA. For the evaluation of DNA immunoprecipitated with H3mK27 antibody, the results were presented as a percentage of immunoprecipitation, calculated by dividing the average value of immunoprecipitated DNA by the average value of the corresponding input DNA. Each experiment was performed three times with independent chromatin extracts. The primers used for real-time PCR were primers Q-ChIP1F and Q-ChIP1R for CG11 analysis and primers Q-ChIP2F and Q-ChIP2R for CG12 analysis. The primers for *Gapdh* and *D13Mit55* have been described elsewhere (16).

**Hot-stop PCR and SSCP analysis.** Hot-stop PCR was performed for the analysis of allele-specific histone modifications as follows. After a number of PCR cycles sufficient to detect a product using primers ChIP2F-1 and ChIP2R-1, primer ChIP2R-1 labeled by [ $\gamma$ -<sup>32</sup>P]ATP was added to the mixture, and then one cycle of PCR was performed. The PCR products were digested with the restriction endonuclease Hpy188I and electrophoresed in a 4% polyacrylamide gel. Single-strand conformation polymorphism (SSCP) analysis of PCR products was performed for allele-specific histone methylation in the presence of [ $\gamma$ -<sup>32</sup>P]ATP-labeled primers ChIP2F-2 and ChIP2R-2. PCR products were resolved by electrophoresis in an MDE nondenaturing acrylamide gel (FMC BioProduct, Rockland, ME).

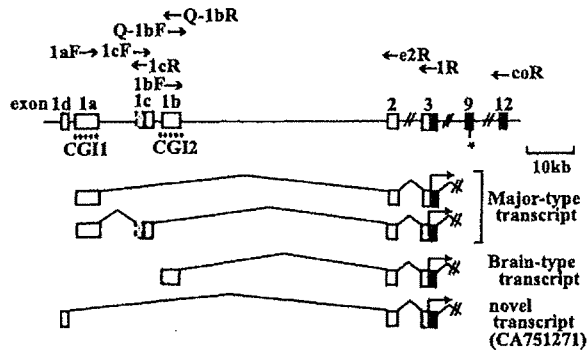


FIG. 1. Tissue-specific transcripts of *Grb10*. Filled boxes, open boxes, and shaded boxes represent protein-coding regions, 5' untranslated regions, and extended exons 1c, respectively. The dashed lines indicate the CpG islands (CGI1 and CGI2) in the promoters. The primers used for RT-PCR are shown. The asterisk indicates the polymorphic site (G/A) between the C57BL/6 and PWK strains.

Primers. The primers used for the analysis are listed in Table 1.

## RESULTS

Mouse *Grb10* has several tissue-specific promoters. Three different promoters of *Grb10* have previously been reported to initiate tissue-specific transcripts (Fig. 1). We first analyzed the expression of each transcript in E16 fetal tissues. The major-type transcript amplified by PCR using primers 1aF and e2R in exons 1a and 2, respectively, was detected in the fetal brain but was less detected in other tissues, while the brain type transcript amplified by primers 1bF and e2R in exons 1b and 2, respectively, was detected exclusively in the fetal brain (Fig. 2A). Another transcript which was previously reported to be brain specific in adult tissues (1) was examined in fetal tissues. PCR using primers 1cF and e2R in exons 1c and 2, respectively, showed that exon 1c was expressed not only in the fetal brain but also in the fetal liver and kidney (Fig. 2A). To assess whether exon 1c is an alternatively spliced exon of the major-type transcript with exon 1a, we performed PCR using primers 1aF and 1cR in exons 1a and 1c, respectively. The PCR product containing exons 1a and 1c was detected in the fetal tissues (Fig. 2A). Sequence analysis of the RT-PCR product revealed that exon 1c was extended 67 bp upstream of the previously published exon 1c with the consensus splicing site (Fig. 1). Any RT-PCR products with both exons 1a and 1b or both exons 1c and 1b were not found (data not shown). Furthermore, we identified another putative exon, 1d, located 1.2 kb upstream of exon 1a in the expressed sequence tag database (GenBank accession no. CA751271). The existence of the novel exon 1d was confirmed by RT-PCR in the embryonic liver but not in other tissues, including the brain (data not shown).

**Expression of *Grb10* shifts from the major-type to the brain type transcript during brain development.** To confirm whether the expression level of the brain type transcript changes during brain development, the major-type and brain type transcripts arising from exons 1a and 1b, respectively, were quantitatively analyzed at various developmental stages of the brain. Real-time PCR analysis showed that in the brain, the major-type transcript was highly expressed at E10 and decreased accord-

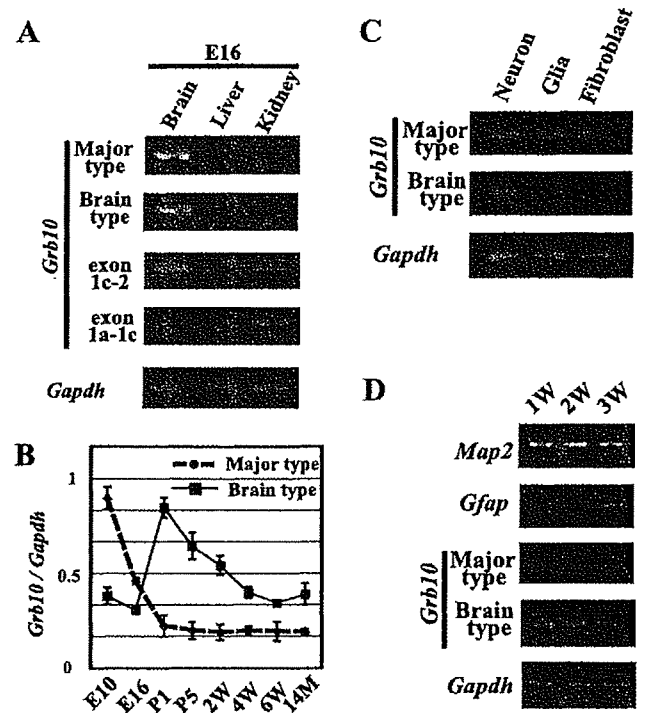


FIG. 2. Expression analysis of each transcript in embryonic tissues by RT-PCR. (A) Semiquantitative analysis of tissues from the E16 embryo. Exon 1c-2 and exon 1a-1c represent RT-PCR products amplified by primer sets 1cF/e2R and 1aF/1cR, respectively. The concentration of each cDNA was adjusted for *Gapdh* amplification as an internal control. (B) Quantitative evaluation of major-type and brain type transcripts in brain tissues from different developmental stages by real-time PCR. The relative amounts of major-type and brain type transcripts are shown. The relative amount of each transcript was calculated by normalizing each value with an internal control, *Gapdh*. Standard errors of the means are indicated by bars. (C) Expression analysis of major-type and brain type transcripts in the primary cell culture. (D) Evaluation of expression of marker genes and each *Grb10* transcript according to the culture period. 1w (1 week), 2w (2 weeks), and 3w (3 weeks) indicate the periods of neuron culture. P1, postnatal day 1; 14M, 14 months.

ing to brain development, while expression of the brain type transcript was high in the perinatal period and gradually decreased thereafter (Fig. 2B). The result indicates that *Grb10* transcripts shift from the major type to the brain type during early brain development.

**The brain-specific transcript is expressed in neurons but not in glial cells.** Is the brain type transcript expressed exclusively in the brain restricted to the cell type? To know which type of brain cells, neurons or glial cells, express the brain type transcript, expression analysis of cultured neurons and glial cells was carried out. Prior to the analysis, we confirmed by immunostaining and RT-PCR with the brain precursors, neuronal and glial markers, that over 95% of the two cultured cell types were postmitotic neurons and astrocytes, respectively (data not shown). RT-PCR in cultured cells revealed that the major-type transcript was expressed in all cultured brain cells but that the brain type transcript was expressed only in neurons (Fig. 2C). We next tried to investigate whether these transcripts in the brain were associated with the maturation of

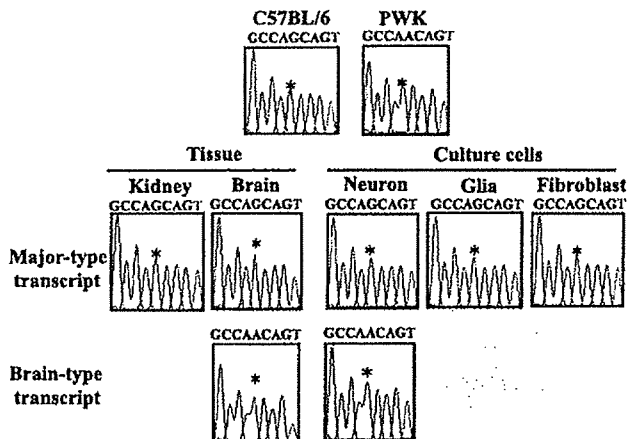


FIG. 3. Imprinting analysis of promoter-specific expression of *Grb10* by sequence chromatograms. Upper panels show the chromatograms of the genomic PCR products from each strain. Middle and lower panels show the chromatograms of the RT-PCR products from tissues and cultured cells of the  $F_1$  hybrid, in which alleles were distinguished by the single-nucleotide (G/A) polymorphism (\*) at exon 9.

neurons. Neurons were cultured for 1, 2, and 3 weeks, and semiquantitative RT-PCR was carried out. Before expression analysis of *Grb10*, the status of cell proliferation and differentiation by long culture was evaluated by primers for *Map2* as a marker for neurons and *Gfap* as a marker for astrocytes under the normalization of cDNA concentration to *Gapdh* (Fig. 2D). The expression of *Map2* never changed in 3-week-cultured cells, while that of *Gfap* was detected in the cells cultured for 3 weeks. In these long-culture cells, the brain type transcript was continuously expressed during culture periods, while the major-type transcript was less expressed than the brain type transcript. These results suggest that both types of transcripts are expressed in neurons and that the switching of the promoter from the major type to the brain type is observed during long culture periods.

#### Promoter-specific paternal expression of *Grb10* in the brain.

To investigate the imprinted expression of *Grb10*, we first examined parental expression of the major-type and the brain type transcripts in the brain and kidney from  $F_1$  hybrid mice by direct sequencing of the RT-PCR product. A polymorphic site (G/A) in exon 9 between the C57BL/6 and PWK strains was used to determine the paternal allele (Fig. 1). As previously reported by Hikichi et al. (17), the major-type transcript was expressed exclusively from the maternal allele in the kidney and brain, while the brain type transcript was expressed from the paternal allele only in the brain (Fig. 3). We next examined promoter-specific imprinting in neurons, glial cells, and fibroblasts. Expression of the major-type transcript originated exclusively from the maternal allele in all cultured cells, but that of the brain type transcript detected only in neurons originated from the paternal allele (Fig. 3). Thus, predominant paternal *Grb10* expression in the brain, as previously described, can be explained by a combination of paternally expressed brain type transcript in neurons and maternally expressed major-type transcript in all cells.

**Differentially methylated CGI2 is maintained in cultured neurons and glial cells.** As we found that the brain type tran-

script was initiated from exon 1b of the paternal allele only in neurons, we analyzed the methylation status of the brain type promoter in neurons and glial cells by the bisulfite method. As shown in Fig. 4A, three promoters are located within different CGIs: exon 1a in CGI1, exon 1b in CGI2, and exon 1c in the "weaker" CpG island, CGI3. The parental origin of the methylated allele was identified by polymorphic sites in  $F_1$  hybrids between the C57BL/6 and PWK strains. The methylation analysis of CGI2 showed that the differential methylation established in the germ cells (1, 17) was maintained in neurons and glial cells (Fig. 4B). That in other CpG islands, CGI1 and CGI3, revealed biallelic hypomethylation and hypermethylation, respectively. CGI1 and CGI3 did not show any differential methylation in the cells, although CGI3 was reported to be a putative differentially methylated region in the mouse brain with uniparental disomy for chromosome 11 (1). The methylation status in CGIs, except CGI3, in cultured cells was consistent with that previously reported for tissues (1, 17).

**Parental chromosome-specific histone modifications in CGI2 correlate with allele-specific expression of the brain type transcript in neurons.** Parental origin-specific histone modifications are reported to represent the determinant of epigenetic features as well as DNA methylation. Using specific antibodies against acetylated histone H3 (H3Ac), acetylated histone H4 (H4Ac), dimethylated Lys4 histone H3 (H3mK4), and di- and trimethylated Lys9 histone H3 (H3me2K9 and H3me3K9), we performed a ChIP assay with cultured cells. After evaluation of ChIP DNA by allele-specific histone modifications in the *Lit1* promoter region as a control (16), histone modifications in CGI1, CGI2, and CGI3 were analyzed by real-time PCR to quantify their precipitated chromatin in these CGIs. To normalize each value, *Gapdh* and *D13Mit55* were used as internal control sequences, where acetylated and methylated histones were known to be biallelically immunoprecipitated, depending on the corresponding antibodies. In CGI2, where the maternal allele-specific DNA methylation was established in the oocyte, H3Ac, H4Ac, H3mK4, and H3me3K9 were clearly immunoprecipitated in neurons, while in glial cells and fibroblasts, although H3mK4 and H3me3K9 were well immunoprecipitated, H3Ac and H4Ac were less precipitated (Fig. 5A). The results obtained with the antibody against H3me2K9 (data not shown) were similar to those obtained with the antibody against H3me3K9.

To elucidate the parental chromosome-specific histone modifications in CGI2 in neurons, hot-spot PCR was performed (15, 32). The restriction endonuclease Hpy188I was used to recognize the polymorphic site in CGI2. For each of the precipitated samples, the ratio of the paternal to maternal band intensities was determined. These ratios were corrected for the paternal-to-maternal ratios in the input chromatin, because the maternal and paternal alleles were not equally represented in the input chromatin. One of the parental alleles is possibly more sensitive to sonication in these regions because of relaxed chromatin (12, 16, 39). The result revealed that histones H3 and H4 were hyperacetylated and that H3K4 was hypermethylated predominantly on the paternal chromosome (Fig. 5B). To investigate allele-specific histone trimethylation of H3K9 in neurons and fibroblasts, SSCP analysis of PCR products was also performed. In





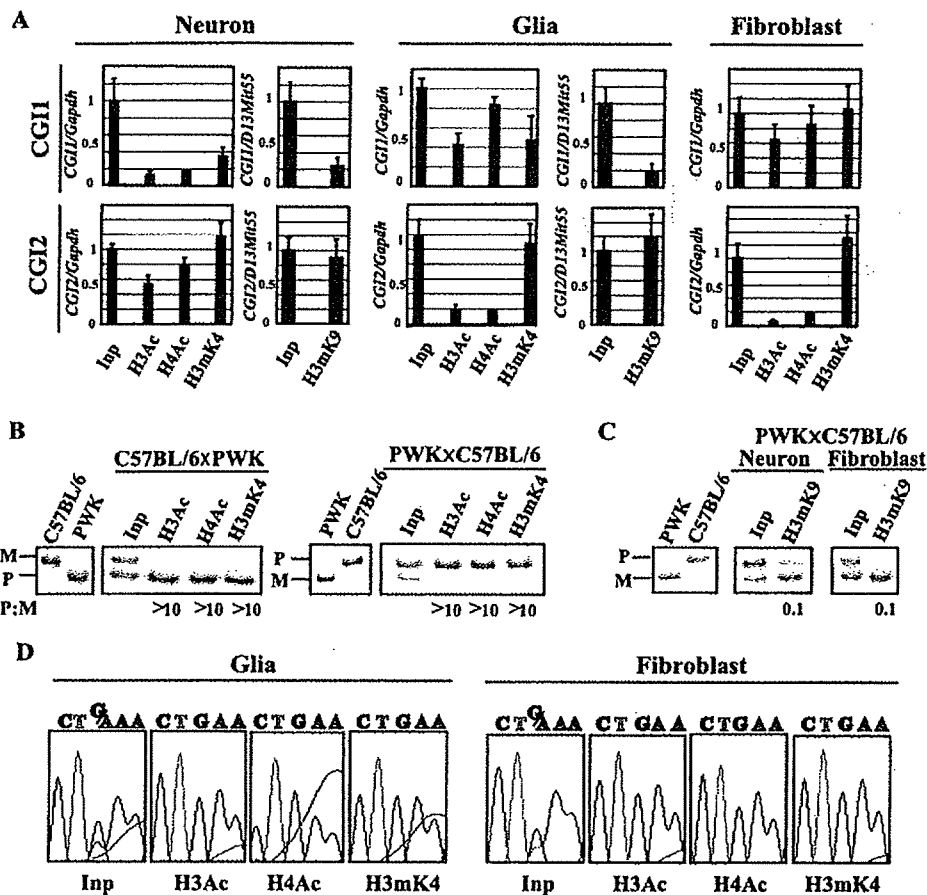


FIG. 5. Histone modification analysis of the *Grb10* promoter in cultured cells. (A) Quantitative analysis of immunoprecipitated DNA by real-time PCR. Quantitative values of precipitated DNA in CGII and CGI2 were normalized by dividing the average value of each CGI by the average value of *Gapdh* or *D13Mit55*. Standard errors of the means are indicated by bars. (B) Allele-specific histone modifications in CGII in neurons by hot-stop PCR. Digested PCR products of C57BL/6 and PWK genomic DNA are shown as homozygous controls in the first two lanes. M and P represent the products from the maternal allele and the paternal allele, respectively. The ratio of the paternal to maternal (P:M) band intensities, corrected by the ratio in input chromatin (Inp), is indicated below each lane. (C) Allele-specific histone H3K9 methylation in CGII by SSCP. PCR products of C57BL/6 and PWK genomic DNA were shown as controls in the first two lanes. (D) Allele-specific histone modifications in CGII by sequence chromatograms. Glial cells and fibroblasts derived from  $F_1$  hybrids [(C57BL/6  $\times$  PWK) $F_1$ ] were used for analysis. The single-nucleotide (G/A) polymorphism is detected in the input sample (Inp); "G" originated from the maternal allele and "A" from the paternal allele.

results in vitro can explain the previous data that the brain type transcript was not detected in whole embryo at E9.5 (17), when neurogenesis has not yet occurred. In addition, our data on *Grb10* expression, i.e., brain development-dependent switching from the major-type to the brain type transcript, can also support the previous report that *Grb10* is expressed predominantly from the paternal allele in the adult brain (17), which consists of neurons and glial cells.

In our expression analysis, we detected both brain type and major-type transcripts in cultured neurons (Fig. 2B). Recently, it was reported that the *Pcdh* (protocadherin) gene was monoallelically expressed in individual neurons (10). The *Pcdh* gene family (*Pcdha*, *Pcdhb*, and *Pcdhc*) has variable exons and alternative splice forms. Esumi et al. analyzed the expression of transcripts in the variable exons of *Pcdha* by using a single-cell RT-PCR approach for the determination of the allelic origin for each variable exon at the individual cell level (10). The

individual cells showed monoallelic expression for each variable exon. In our analysis of *Grb10*, the discrepancy between the modifications in CGII and the expression of the major-type transcript in neurons was recognized. Similar to a monoallelic expression pattern of variable *Pcdha* exons in individual neurons, the discrepancy may be explained by the existence of two different cell populations in cultured neurons, each of which expresses either the major-type or the brain type transcript exclusively. As shown in Fig. 2D, the brain type transcript was obviously highly expressed compared to the major-type transcript during long culture periods. The larger population of cells with the brain type transcript may affect the result of histone modifications more than the smaller population of cells with the major-type transcript.

It has been reported that histone modifications and DNA methylation are not synchronized as a transcriptionally active/silent signal in some imprinted genes, such as *NDN*, *Gnas*, and

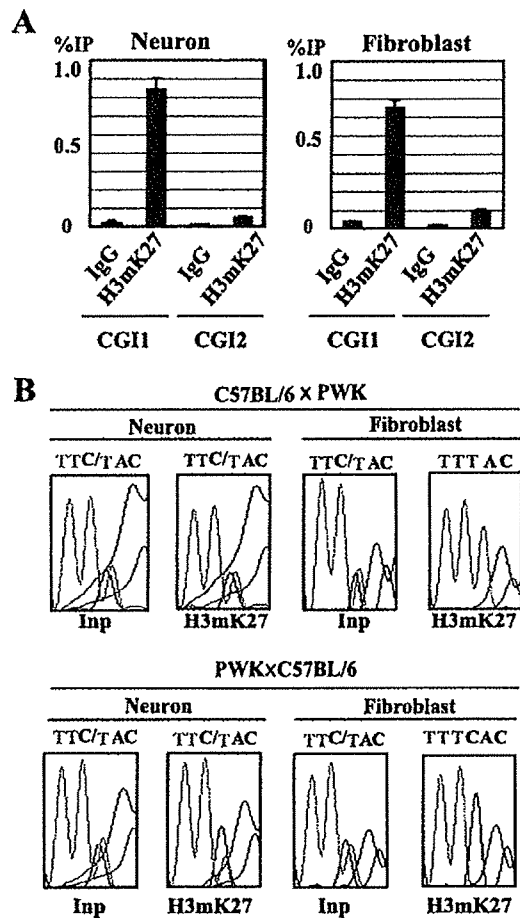


FIG. 6. Histone H3K27 methylation analysis of CG11 and CG12 in cultured cells. (A) Quantitative analysis of immunoprecipitated DNA by real-time PCR. The percentage of immunoprecipitation (IP) was calculated by dividing the quantitative value of precipitated DNA by that of the corresponding input DNA. Standard errors of the means are indicated by bars. (B) Allele-specific histone modifications in CG11 by sequence chromatograms. Neurons and fibroblasts derived from F<sub>1</sub> hybrids (C57BL/6 × PWK; PWK × C57BL/6) were used for analysis. The single-nucleotide (C/T) polymorphism is detected in the input sample (Inp); "C" originated from the C57BL/6 allele and "T" from the PWK allele. IgG, immunoglobulin G.

*Igf2r* (21, 22, 23, 33, 35). Our data also showed an epigenetically unsynchronized active/silent signal between DNA methylation and histone modifications in *Grb10* (Fig. 7). In this study, we showed that the brain type transcript is expressed in neurons but not in glial cells (Fig. 2C), where both differential methylation in CG12 and biallelic hypomethylation in CG11 were maintained regardless of expression (Fig. 4B). The result that allele-specific DNA methylation is not sufficient to direct imprinted expression in brain cells implies that other epigenetic modifications may affect cell lineage-specific imprinting.

In our analysis of histone modifications, histone acetylation status correlated with the expression status of the major-type transcript in glial cells and fibroblasts and the brain type transcript in neurons (Fig. 7). Such histone acetylation status in *Grb10* expression is consistent with the findings that allele-specific histone acetylation was associated with allelic gene expression in the imprinted gene, *NDN* (21). Histone acetylation offers the best example of a direct link between tissue-specific gene expression and histone modifications.

Unlike that of histone acetylation, the status of histone methylation has been implicated as an early event for chromatin conformations. Methylation of histones H3K4 and H3K9 is associated with active chromatin and silent chromatin, respectively. According to our results, allele-specific H3K4 and H3K9 methylation in CG11 and CG12 did not correlate with allele-specific gene expression in each cultured cell. In glial cells, H3K4 in CG12 was hypermethylated in the paternal chromosome, which was silent with no brain type transcript. It seems that H3mK4 is maintained during differentiation as an imprint mark with H3mK9 but is not related to promoter activity (28), although histone modifications in oocytes remain unknown. In CG11, H3me2K9 and H3me3K9 were hypomethylated in both parental chromosomes independent of the expression of the major-type transcript in cultured cells. It is likely that H3K9 methylation in germ cells is maintained as a stable and heritable imprint mark but may not be secondarily acquired during development.

Then, how is maternal chromosome-specific expression of the major-type transcript regulated without differential DNA methylation in CG11? The PcG protein Eed complex is known to be a part of a memory system that maintains repression of

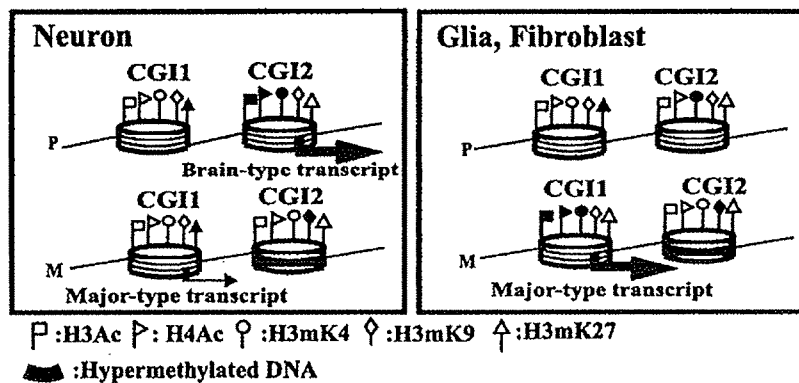


FIG. 7. Summary of epigenetic modifications across promoter regions of *Grb10*. M and P represent maternal and paternal chromosomes, respectively. Large and small arrows indicate expression levels. The nucleosome model shows DNA wrapping around a histone octamer with some histone modifications. White and black flags represent hypoacetylated/hypomethylated and hyperacetylated/hypermethylated statuses, respectively.

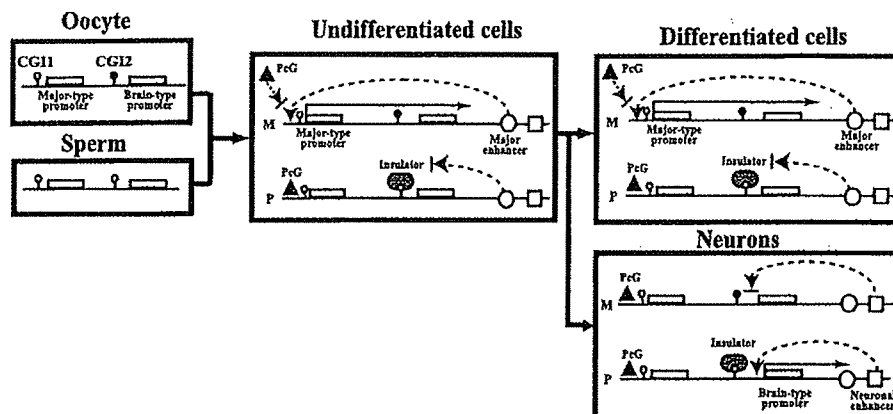


FIG. 8. Working models for tissue-specific reciprocal imprinting of *Grb10*. The previous enhancer/insulator model by Hikichi et al. was modified based on the analysis of DNA methylation and histone modifications mediated by the PcG complex containing Eed (17). Tissue-specific imprinting of *Grb10* implies neuron-specific imprinting that is different from imprinting in other undifferentiated and differentiated cells. Black and white lollipops indicate hypermethylated and hypomethylated DNA, respectively. Circles and squares indicate putative major enhancer and neuronal enhancer, respectively, which accelerate *Grb10* expression from the major-type promoter and the brain type promoter, respectively. The PcG complex containing Eed is represented by a triangle. CTCF is thought to be a putative insulator (gray oval). M, maternal; P, paternal.

the imprinted X chromosome (36) and silencing of some imprinted genes (24, 33). *Grb10* is reported to be one of the imprinted genes that are regulated by the PcG protein Eed complex. Interestingly, in *Eed*<sup>-/-</sup> embryos, the major-type transcript was biallelically expressed without major alteration of allelic DNA methylation (24). The Eed/Ezh2 PcG complex possesses histone methyltransferase activity on H3K27 (5, 8, 25) and interacts with histone deacetylases (34). Methylation of H3K27 is a repressive epigenetic mark regulated by the SET domain containing Ezh2/Eed complex (5, 8, 20, 25). In our analysis, H3mK27 was clearly precipitated in neurons and fibroblasts in CGI1 but not in CGI2 (Fig. 6A). The paternal chromosome-specific methylation of H3K27 in CGI1 was observed in fibroblasts but not in neurons (Fig. 6B). These data indicate that the Eed PcG complex can biallelically interact on CGI1 as a *trans*-acting factor in neurons but paternally in other cells. In the absence of DNA methylation in CGI1, PcG complexes may mediate a nonpermissive chromatin state for transcription, leading to repressive histone modifications. Interestingly, other genes, *Cdkn1c* and *Ascl2*, imprinting of which was reported to be regulated by Eed (24), show tissue-specific imprinting, and their imprinted expression in trophoblasts is associated with repressive histone H3K27 methylation rather than DNA methylation (22, 33).

Figure 7 shows the summary of our data. In CGI2, DNA methylation in a gametically methylated CpG island on the maternal allele was maintained throughout development. Allelic methylation of H3K4 and H3K9 associated with gametic DNA methylation was also stable as an epigenetic mark, independent of *Grb10* expression. Histone acetylation status was correlated with the expression status of the brain type transcript: histones H3 and H4 were paternally acetylated only in neurons, where the brain type transcript was paternally expressed. H3K27 was not methylated biallelically. In CGI1, biallelic DNA hypomethylation and biallelic hypomethylation of H3K9 were observed. Acetylation of histones H3 and H4 and methylation of H3K4 and H3K27 were allelically detected,

corresponding to the allelic expression of the major-type transcript, although the discordance in histone modifications and expression in neurons was detected, probably depending on maturation of neurons. Methylation of H3K9 and H3K27 is thought to be a repressive chromatin marker, but it is not completely clear whether PcG-mediated silencing involves methylation of H3K9 synchronized with H3mK27 in all PcG target genes. We did not observe coexistence of H3mK27 and H3mK9 in both CGI1 and CGI2 of *Grb10*. Umlauf et al. also reported discordance between localizations of H3mK27 and H3mK9 in some imprinted genes in the *Kcnq1* domain (33). Further work should determine how histone modifications, especially methylation of H3K9 and H3K27, are coordinated or uncoordinated as epigenetic determinants in tissue-specific imprinting.

These data about epigenetic modifications analyzed at the cell level, in addition to the evidence for *Dnmt3L*<sup>m-/-</sup> and *Eed*<sup>-/-</sup> embryos, lead to a working model for tissue-specific reciprocal imprinting of *Grb10* (Fig. 8). The previous model by Hikichi et al. (17) was modified in our model based on the data of DNA methylation and repressive histone modifications mediated by the PcG complex in brain cell lineages. In undifferentiated cells, a DNA methylation-sensitive insulator, CTCF, binds to the paternal CGI2 and blocks the paternal activity of the downstream major enhancer, resulting in silent expression of the major-type transcript on the paternal allele. On the maternal allele, the major enhancer works on the major-type promoter to recruit transcription factors. In CGI1, the Eed/Ezh2 PcG complex binds on the paternal allele, whereas it competes with transcription factors on the maternal allele. The Eed/Ezh2 PcG complex methylates H3K27 and interacts with histone deacetylases, leading to silencing of the chromatin on the paternal CGI1. In *Dnmt3L*<sup>m-/-</sup> embryos, biallelic hypomethylation in CGI2 makes CTCF bind biallelically on CGI2, resulting in null expression of the major-type transcript, regardless of the PcG complex. In *Eed*<sup>-/-</sup> embryos, the silent state on the paternal CGI1 regulated by the Eed PcG complex

is released to the biallelically active state without major alteration of DNA methylation in maternal CGI2. In neurons, the other molecular mechanism of imprinting works in a promoter-specific manner, different from that in other differentiated cells. During neurogenesis, expression of *Grb10* shifts from the major-type to the brain type transcript by switching from the major-type promoter to the brain type promoter. The neuronal enhancer instead of the major enhancer may work on the brain type promoter, depending on DNA methylation in CGI2. The maternally active major-type promoter becomes silent without transcription factors, and consequently, the Eed/Ezh2 PcG complex binds to make the chromatin structure silent. This implies that the PcG complex is necessary to maintain cell-type-specific imprinting. It remains unknown how neuron-specific imprinting is regulated by DNA methylation and/or histone modifications mediated by the PcG complex, because *Dnmt3L*<sup>m-/-</sup> and *Eed*<sup>-/-</sup> embryos are lethal by E10.5 (4, 14) and E8.5 (11), respectively, just before neurogenesis.

As far as we know, this is the first report of an epigenetic analysis of cultured cells where DNA methylation and chromatin remodeling by PcG proteins establish and maintain cell-type-specific imprinting at one gene locus. Although allelic DNA methylation established in the gamete contributes primarily to tissue-specific imprinting, tissue-specific *Grb10* imprinting is directly regulated by the repressive chromatin mediated by the PcG complex during development. Our analysis of promoter-specific and cell-type-specific imprinting of *Grb10* gives an important clue for understanding the mechanism of tissue-specific imprinting.

#### ACKNOWLEDGMENTS

We thank F. Ishino for providing information about genomic sequences of *Grb10* promoter regions.

T.K. was supported in part by a Grant-in-Aid for Scientific Research (C) and a Grant-in-Aid on Priority Areas (Molecular Brain Science) from the Ministry of Education, Culture, Sports, Science and Technology of Japan.

#### REFERENCES

- Arnaud, P., D. Monk, M. P. Hichins, E. Gordon, W. Dean, C. Beechey, J. Peters, W. Craigen, M. Preece, P. Stanier, G. E. Moore, and G. Kelsey. 2003. Conserved methylation imprints in the human and mouse GRB10 genes with divergent allelic expression suggests differential reading of the same mark. *Hum. Mol. Genet.* 12:1005-1019.
- Arnaud, P., K. Hata, M. Kaneda, E. Li, H. Sasaki, R. Feil, and G. Kelsey. 2006. Stochastic imprinting in the progeny of *Dnmt3L*<sup>-/-</sup> females. *Hum. Mol. Genet.* 15:589-598.
- Bantignies, F., and G. Cavalli. 2006. Cellular memory and dynamic regulation of Polycomb group proteins. *Curr. Opin. Cell Biol.* 18:1-9.
- Bourc'his, D., G. L. Xu, C. S. Lin, B. Bollman, and T. H. Bester. 2001. *Dnmt3L* and the establishment of maternal genomic imprints. *Science* 294:2536-2539.
- Cao, R., L. Wang, H. Wang, L. Xia, H. Erdjument-Bromage, P. Tempst, R. S. Jones, and Y. Zhang. 2002. Role of histone H3 lysine 27 methylation in Polycomb-group silencing. *Science* 298:1039-1043.
- Cattanach, B. M., and C. V. Beechey. 1990. Autosomal and X-chromosome imprinting. *Dev. Suppl.* 1990:63-72.
- Constancia, M., B. Pickard, G. Kelsey, and W. Reik. 1988. Imprinting mechanisms. *Genome Res.* 8:881-900.
- Czermin, B., R. Melfi, D. McCabe, V. Seitz, A. Imhof, and V. Pirrotta. 2002. *Drosophila* enhancer of Zeste/ESC complexes have a histone H3 methyltransferase activity that marks chromosomal Polycomb sites. *Cell* 111:185-196.
- Davies, W., A. R. Isles, and L. S. Wilkinson. 2005. Imprinted gene expression in the brain. *Neurosci. Biobehav. Rev.* 29:421-430.
- Esumi, S., N. Kakazu, Y. Taguchi, T. Hirayama, A. Sasaki, T. Hirabayashi, T. Koide, T. Kitsukawa, S. Hamada, and T. Yagi. 2005. Monoallelic yet combinatorial expression of variable exons of the protocadherin-a gene cluster in single neurons. *Nat. Genet.* 37:171-176.
- Faust, C., A. Schumacher, B. Holdener, and T. Magnuson. 1995. The *eed* mutation disrupts anterior mesoderm production in mice. *Development* 121:273-285.
- Fournier, C., Y. Goto, E. Ballestar, K. Delaval, A. M. Hever, M. Esteller, and R. Feil. 2002. Allele-specific histone lysine methylation marks regulatory regions at imprinted mouse genes. *EMBO J.* 21:6560-6570.
- Gregory, R. I., T. E. Randall, C. A. Johnson, S. Khosla, I. Hatada, L. P. O'Neill, B. M. Turner, and R. Feil. 2001. DNA methylation is linked to deacetylation of histone H3, but not H4, on the imprinted genes *Snrpn* and *U2af1-rs1*. *Mol. Cell. Biol.* 21:5426-5436.
- Hata, K., M. Okano, H. Lei, and E. Li. 2002. *Dnmt3L* cooperates with the *Dnmt3* family of de novo DNA methyltransferases to establish maternal imprints in mice. *Development* 129:1983-1993.
- Higashimoto, K., H. Soejima, H. Yatsuki, K. Joh, M. Uchiyama, Y. Obata, R. Ono, Y. Wang, Z. Xin, X. Zhu, S. Masuko, F. Ishino, I. Hatada, Y. Jinno, T. Iwasaka, T. Katsuki, and T. Mukai. 2002. Characterization and imprinting status of *OBPH1/Obph1* gene: implications for an extended imprinting domain in human and mouse. *Genomics* 80:575-584.
- Higashimoto, K., T. Urano, K. Sugiura, H. Yatsuki, K. Joh, W. Zhao, M. Iwakawa, H. Ohashi, M. Oshimura, N. Niikawa, T. Mukai, and H. Soejima. 2003. Loss of CpG methylation is strongly correlated with loss of histone H3 lysine 9 methylation at DMR-LIT1 in patients with Beckwith-Wiedemann syndrome. *Am. J. Hum. Genet.* 73:948-956.
- Hikichi, T., T. Kohda, T. Kaneko-Ishino, and F. Ishino. 2003. Imprinting regulation of the murine *Meg1/Grb10* and human *GRB10* genes; roles of brain-specific promoters and mouse-specific CTCF-binding sites. *Nucleic Acids Res.* 31:1398-1406.
- Kaneda, M., M. Okano, K. Hata, T. Sado, N. Tsujimoto, E. Li, and H. Sasaki. 2004. Essential role for de novo DNA methyltransferase *Dnmt3a* in paternal and maternal imprinting. *Nature* 429:900-903.
- Kishino, T. 2006. Imprinting in neurons. *Cytogenet. Genome Res.* 113:209-214.
- Kuzmichev, A., K. Nishioka, H. Erdjument-Bromage, P. Tempst, and D. Reinberg. 2002. Histone methyltransferase activity associated with a human multiprotein complex containing the Enhancer of Zeste protein. *Genes Dev.* 16:2893-2905.
- Lau, J. C., M. L. Hanel, and R. Wevrick. 2004. Tissue-specific and imprinted epigenetic modifications of the human *NDN* gene. *Nucleic Acids Res.* 32:3376-3382.
- Lewis, A., K. Mitsuya, D. Umlauf, P. Smith, W. Dean, J. Walter, M. Higgins, R. Feil, and W. Reik. 2004. Imprinting on distal chromosome 7 in the placenta involves repressive histone methylation independent of DNA methylation. *Nat. Genet.* 36:1291-1295.
- Li, T., T. H. Vu, G. A. Ulaner, Y. Yang, J. F. Hu, and A. R. Hoffman. 2004. Activating and silencing histone modifications from independent allelic switch regions in the imprinted *Gnus* gene. *Hum. Mol. Genet.* 13:741-750.
- Mager, J., N. D. Montgomery, F. P. de Villena, and T. Magnuson. 2003. Genome imprinting regulated by the mouse Polycomb group protein Eed. *Nat. Genet.* 33:502-507.
- Muller, J., C. M. Hart, N. J. Francis, M. L. Vargas, A. Sengupta, B. Wild, E. L. Miller, M. B. O'Connor, R. E. Kingston, and J. A. Simon. 2002. Histone methyltransferase activity of a *Drosophila* Polycomb group repressor complex. *Cell* 111:197-208.
- Nakagawachi, T., H. Soejima, T. Urano, W. Zhao, K. Higashimoto, Y. Satoh, S. Matsukura, S. Kudo, Y. Kitajima, H. Harada, K. Furukawa, H. Matsuzaki, M. Emi, Y. Nakabeppu, K. Miyazaki, M. Sekiguchi, and T. Mukai. 2003. Silencing effect of CpG island hypermethylation and histone modifications on O6-methylguanine-DNA methyltransferase (*MGMT*) gene expression in human cancer. *Oncogene* 22:8835-8844.
- Pirrotta, V. 1995. Chromatin complexes regulating gene expression in *Drosophila*. *Curr. Opin. Genet. Dev.* 5:466-472.
- Rougeulle, C., P. Navarro, and P. Avner. 2003. Promoter-restricted H3 Lys 4 di-methylation is an epigenetic mark for monoallelic expression. *Hum. Mol. Genet.* 12:3343-3348.
- Saitoh, S., and T. Wada. 2000. Parent-of-origin specific histone acetylation and reactivation of a key imprinted gene locus in Prader-Willi syndrome. *Am. J. Hum. Genet.* 66:1958-1962.
- Surani, M. A., S. C. Barton, and M. L. Norris. 1984. Development of reconstituted mouse eggs suggests imprinting of the genome during gametogenesis. *Nature* 308:548-550.
- Tilghman, S. M. 1999. The sins of the fathers and mothers: genomic imprinting in mammalian development. *Cell* 96:185-193.
- Uejima, H., M. P. Lee, H. Cui, and A. P. Feinberg. 2000. Hot-stop PCR: a simple and general assay for linear quantitation of allele ratios. *Nat. Genet.* 25:375-376.
- Umlauf, D., Y. Goto, R. Cao, F. Cerqueira, A. Wagschal, Y. Zhang, and R. Feil. 2004. Imprinting along the *Kcnq1* domain on mouse chromosome 7 involves repressive histone methylation and recruitment of Polycomb group complexes. *Nat. Genet.* 36:1296-1300.
- van der Vlag, J., and A. P. Otte. 1999. Transcriptional repression mediated by the human polycomb-group protein EED involves histone deacetylation. *Nat. Genet.* 23:474-478.
- Vu, T. H., T. Li, and A. R. Hoffman. 2004. Promoter-restricted histone code,